

# ACCOR: Attention-Enhanced Complex-Valued Contrastive Learning for Occluded Object Classification Using mmWave Radar IQ Signals

Stefan Hägele, Adam Misik, Constantin Patsch, and Eckehard Steinbach

**Abstract**—Millimeter-wave (mmWave) radar has emerged as a robust sensing modality for several areas, offering reliable operation under adverse environmental conditions. Its ability to penetrate lightweight materials such as packaging or thin walls enables non-visual sensing in industrial and automated environments and can provide robotic platforms with enhanced environmental perception when used alongside optical sensors. Recent work with MIMO mmWave radar has demonstrated its ability to penetrate cardboard packaging for occluded object classification. However, existing models leave room for improvement and warrant a more thorough evaluation across different sensing frequencies. In this paper, we propose ACCOR, an attention-enhanced complex-valued contrastive learning approach for radar, enabling robust occluded object classification. We process complex-valued IQ radar signals using a complex-valued CNN backbone, followed by a multi-head attention layer and a hybrid loss. Our proposed loss combines a weighted cross-entropy term with a supervised contrastive term. We further extend an existing 64 GHz dataset with a 67 GHz subset of the occluded objects and evaluate our model using both center frequencies. Performance evaluation demonstrates that our approach outperforms prior radar-specific models and image classification models with adapted input, achieving classification accuracies of 96.60% at 64 GHz and 93.59% at 67 GHz for ten different objects. These results demonstrate the benefits of complex-valued deep learning with attention and contrastive learning for mmWave radar-based occluded object classification in industrial and automated environments.

The dataset can be found at <https://github.com/haegels/radar-IQ-datasets#>.

The new sub-dataset will be published upon the paper's acceptance.

## I. INTRODUCTION

In recent years, millimeter-wave (mmWave) radar has gained increasing popularity across various sensing domains. Due to its low cost and wide availability, it provides robust performance in applications such as automotive, tracking, human activity- or gesture recognition, or robot perception. Moreover, mmWave radar is often integrated into sensor fusion frameworks to enhance perception, particularly in automotive systems [1], [2], [3], [4], [5], [6], [7], [8]. Unlike optical sensors such as LiDAR or RGB cameras, mmWave

The authors Stefan Hägele, Adam Misik, Constantin Patsch, and Eckehard Steinbach are with the *Chair of Media Technology, School of Computation, Information and Technology, Technical University of Munich and the Munich Institute of Robotics and Machine Intelligence*.

{stefan.haegele, adam.misik, constantin.patsch, eckehard.steinbach}@tum.de

Corresponding author: Stefan Hägele

The authors acknowledge the financial support by the Federal Ministry of Research, Technology and Space of Germany in the programme of “Souverän. Digital. Vernetzt.”. Joint project 6G-life, project identification number: 16KISK002

radar operates reliably under adverse environmental conditions including fog, smoke, rain, or complete darkness, where optical methods typically degrade [9], [10], [11], [12]. This enables more robust perception across all fields mmWave radar sensors are employed. Furthermore, operating in the 30–300 GHz range of the non-visible electromagnetic spectrum, it can penetrate lightweight, non-metallic, and weakly reflective materials such as fabric, cardboard, or plastic. This property provides robust mmWave radar-based perception for occluded object classification, making it well-suited for applications such as automated inspection, concealed object detection, and inventory management in industrial environments. In conveyor belt setups, mmWave radar can identify packaged objects, allowing robots to handle sorting, inspection, and further processing - capabilities that conventional optical sensors cannot generally provide. Existing radar-based concealed object classification methods, however, remain constrained by their reliance on large-scale antenna array imaging scanners, either physical or virtual, which limits their scalability for compact industrial automation systems [13], [14]. These approaches also typically require manual inspection or image-processing algorithms for object detection and classification. As a first step toward more practical solutions, [15] demonstrated that occluded object detection and classification can be achieved using a compact and cheap mmWave MIMO radar, direct IQ signal processing (rather than range-Doppler- or range-angle map processing) and a learning-based classification approach. By employing different Convolutional Neural Network (CNN) architectures designed to process complex-valued IQ radar signals, it was shown that occluded objects within packaging boxes can be successfully classified. However, the use of 3D convolutions in their best-performing model introduces a significant computational cost and the dataset is limited with data from one frequency band. Despite recent progress, IQ signal-based approaches have not been systematically examined across different frequency bands. To address this gap, we introduce ACCOR, a deep learning model that integrates complex-valued processing with an attention mechanism and a hybrid loss function, along with new data for studying frequency-dependent penetrability. Specifically, we propose a compact complex-valued CNN backbone, inspired by [16], with an integrated self-attention mechanism to refine critical IQ signal features. The network is trained using a hybrid loss that combines a cross-entropy- and a supervised contrastive loss to enhance class separability and overall classification performance, which is beneficial given that radar signals are inherently very similar to one another. The proposed

framework aims to improve both efficiency and robustness, enabling compact occluded object classification and advancing compact mmWave radar toward practical deployment in industrial automation and logistics. The findings of this work can be carried forward to develop a compact automated radar-based perception system for any industrial setup.

Our contributions are as follows:

- We design a compact complex-valued CNN backbone with integrated self-attention, tailored to exploit amplitude- and phase information in radar IQ signals.
- We introduce a hybrid loss function that combines cross-entropy with supervised contrastive learning, improving class separability and overall classification accuracy.
- We extend existing benchmarks with a new sub-dataset collected at 67 GHz, enabling the first comparative analysis of frequency-dependent penetrability for occluded object classification.

The remainder of this paper is organized as follows: Section II reviews related work in mmWave radar. Section III presents the proposed methodology, while Section IV reports results and model comparisons. Finally, Section V concludes the paper and discusses potential directions for future research.

## II. RELATED WORK

As mentioned, radar, and especially mmWave radar, has gained considerable attention in the last decade. One reason is the increasing availability of compact, high-precision radar solutions on the market. The automotive sector remains the largest application domain for mmWave radar, where its robustness under adverse conditions such as rain and fog makes it a valuable complement to camera and LiDAR sensors for reliable perception [7], [8], [9], [17]. While cameras and LiDAR degrade significantly under such adverse conditions, radar can still perceive the environment due to its ability to penetrate lightweight materials or particles, such as rain [18]. Furthermore, with Doppler-based processing, mmWave radar is widely used for tracking applications in both indoor and outdoor environments [2], [3], [19]. This is especially appealing since radar naturally preserves privacy compared to camera sensors. Another field of mmWave radar research is human activity understanding and gesture recognition. Like tracking, this area relies on Doppler- or even micro-Doppler processing to gain information about the movement and activities of humans [4], [5], [6], [20], [21]. When very high resolution is required, commonly available radar sensors are limited by their relatively small number of transmit and receive antennas. Since a larger number of antennas provides higher spatial resolution, radar imaging is often achieved synthetically by scanning a large area with a moving radar to form a large virtual antenna array over a certain distance. These virtual arrays can then be exploited for higher-resolution imaging, as demonstrated by approaches such as Synthetic Aperture Radar (SAR) for earth observation [22], [23]. However, this approach can also be applied on a smaller scale using testbeds to scan and

image smaller objects [24], [25]. A remedy to these high-effort imaging techniques is the use of radars with a large number of transmit- and receive antennas, providing many virtual channels without requiring active device movement [26]. Such a sensor was used for the data collection in [15] and is further utilized and extended in this work. Despite the aforementioned advances in mmWave radar, most existing approaches rely on pre-processed range–Doppler or range–angle images, or on CFAR-generated radar point clouds as input to deep learning models. However, research on using directly the down-converted complex-valued radar IQ signal remains limited, especially in combination with deep learning [27], [16], [28]. This is mainly due to the lack of publicly available datasets with complex-valued radar IQ signals, as opposed to their pre-processed counterparts, even though these pre-processing steps commonly remove information for a better visualization of the signal. Furthermore, the penetration ability of mmWave radar applies not only to rain and fog but also to light materials such as cardboard or thin drywall [15], [29], [30]. Due to its popularity surge, mmWave radar also arrived as very helpful perception assistance in robotics and automation, as extensively surveyed in [31]. This includes tasks such as localization, mapping, and object classification across diverse scenarios. Due to its compactness, mmWave radar can be easily deployed on moving platforms such as robots or drones [32], [33]. Beyond traditional supervised learning for radar, recent work has explored contrastive and attention-based models, but their application in mmWave radar remains limited, particularly in IQ data-based processing. However, the information content in IQ signals is expected to be higher than in processed radar maps, suggesting that attention-based and contrastive approaches can extract richer information from the signal. Most contrastive learning research in the radar domain has focused on image-based Synthetic Aperture Radar (SAR) [34], [35]. The same holds for radar transformer models and, more broadly, attention-based radar approaches [7], [8], [36], [37]. To conclude, radar provides significant advantages for industrial automation and logistics, motivating this work on occluded object classification. The IQ data collected in [15] is used in this work, complemented by an additional sub-dataset collected at a different frequency band. Together with an adaptation of the complex-valued CNN introduced in [16], this forms the starting point of the work presented in this paper.

## III. METHODOLOGY

### A. Pre-processing and Setup

The radar sensor used for data collection is a 62–69 GHz frequency-modulated continuous wave (FMCW) MIMO mmWave imaging radar from vayyar and minicircuits [26]. This radar is equipped with 20 transmit (Tx) and 20 receive (Rx) antennas, yielding 400 virtual channels from a single measurement shot. Tx and Rx antennas are arranged in an L-shaped position, which generates the virtual channels depicted in Fig. 1. The transmit signal of a single channel

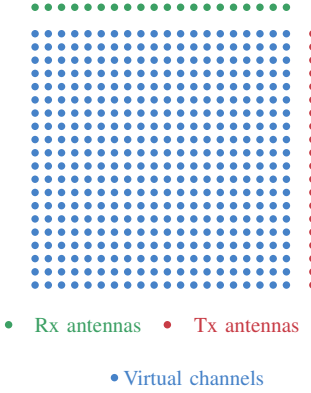


Fig. 1. Virtual channels formed by each antenna pair in the L-shaped  $20 \times 20$  antenna array.

is a FMCW chirp, and can be expressed by the following formula

$$s_c[t] = a[t]e^{j2\pi f_c[t]t}, \quad (1)$$

while every virtual channel in Fig. 1 (blue) is sampled with  $N = 100$  points over one sampling period.  $a[t]$  denotes the amplitude,  $f_c[t]$  the time-dependent frequency, and  $c = 0, 1, 2, \dots, 399$  the channel index. Hence, a single data sample consists of 400 complex-valued IQ signals. The mathematical dimension of a data sample is given by

$$\mathbf{s} \in \mathbb{C}^{(Rx \cdot Tx) \times N}, \quad (2)$$

where  $Rx \cdot Tx = 400$  and  $N = 100$ . To refine the range-specific features of this signal collection, Fourier transform is applied, generating the complex range profile of the FMCW radar IQ signal. Applied as a Fast Fourier Transform (FFT), the one-dimensional Discrete Fourier transform is given by

$$S_c[k] = \sum_{t=0}^{N-1} s_c[t] e^{-j2\pi \frac{kt}{N}}, \quad c = 0, 1, 2, \dots, 399, \quad (3)$$

with  $N = 100$  range bins. For deep learning models such as CNNs, the range profile provides richer and more discriminative features than the raw time-domain IQ signal, as shown in [16]. The schematic setup used for data collection is depicted in Fig. 2, where the distance from sensor to box is around 50 cm. The real setup can be seen in Fig. 3. The box with the occluded object is placed underneath the mmWave sensor and the sample is taken from this position. Due to the penetration capability of mmWave radar, the reflected signal carries information about the object inside the box.

### B. Model Design

1) *CNN and Multi-head Attention*: The backbone of our model is a complex-valued CNN that processes complex-valued input and performs complex-valued operations. Since the FFT-transformed IQ signal is again complex-valued, it is important to extract meaningful features and correspondences from the signal's amplitude and phase, which would be lost using real-valued numbers and operations. Convolutions, batch normalization, and activation functions

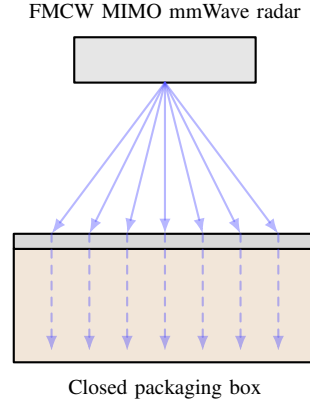


Fig. 2. Sensing Setup: a top-mounted mmWave radar sensing the contents of a closed packaging box.



Fig. 3. Image of the real measurement setup [15].

are all applied in the complex domain [38]. This implies for the convolution of kernel  $k = a + jb \in \mathbb{C}$  and the input  $x = c + jd \in \mathbb{C}$ ,

$$k \cdot x = c \cdot a - d \cdot b + j(c \cdot b + d \cdot a) \quad (4)$$

for the batch normalization (BN) of  $z \in \mathbb{C}$

$$cBN(z) = BN(Re\{z\}) + jBN(Im\{z\}), \quad (5)$$

and for the complex-valued ReLU activation function

$$cReLU(z) \begin{cases} z, & \text{if } Re\{z\}, Im\{z\} \geq 0 \\ 0, & \text{else.} \end{cases} \quad (6)$$

After feature extraction, the features are embedded into a token vector of length  $D = 256$ . Before the projection phase, the complex-valued feature vector is transferred into the real domain. This is achieved by projecting the feature channels into a vector of length 128 and concatenating the real and imaginary parts to obtain a length of  $D$ . This simplifies subsequent processing while preserving the information extracted from the complex-valued backbone. The token vector is then fed into a multi-head self-attention layer with 16 heads. This mechanism is used to refine radar features by enabling the model to capture diverse feature dependencies in range as well as angle domain through multiple parallel attention heads. Fig. 4 presents the overall model architecture, while Fig. 5 illustrates the complex-valued CNN backbone.

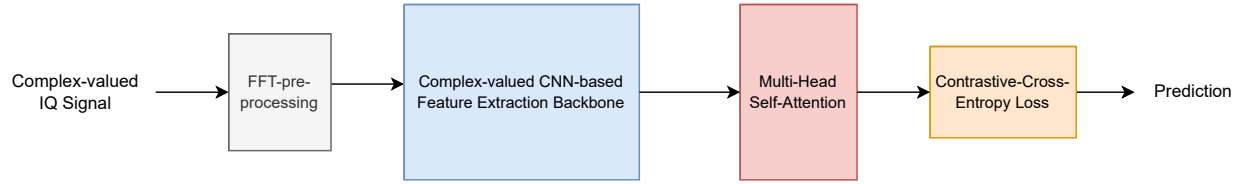


Fig. 4. ACCOR model consisting of FFT pre-processing, a CNN backbone, and a multi-head attention layer, trained with the proposed hybrid loss function.

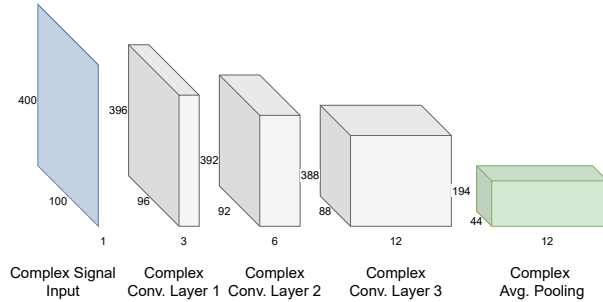


Fig. 5. Complex-valued CNN backbone with three layers and average pooling.

2) *Loss Function*: A hybrid loss function is employed for this classification task. While prior work relied on the standard cross-entropy loss, we adopt a hybrid loss combining weighted cross-entropy loss with contrastive loss, enhancing feature separability and robustness. Since pre-processed radar signals are generally very similar to each other, the contrastive component encourages greater separation of different class samples in the feature space, while the cross-entropy component provides information-theoretically sound label predictions. The formula for the total loss is defined as

$$\ell_{\text{total}} = (1 - \alpha) \ell_{\chi} + \alpha \ell_{\kappa}, \quad (7)$$

where  $\ell_{\chi}$  and  $\ell_{\kappa}$  denote the cross-entropy and contrastive losses, respectively. The parameter  $\alpha$  serves as a tuning factor to assign more weight to one of the losses. Furthermore, the cross-entropy loss  $\ell_{\chi}$  is defined in Eq. 8 and the contrastive loss  $\ell_{\kappa}$  in Eq. 9.

$$\ell_{\chi} = H(\hat{\mathbf{y}}, \mathbf{y}) = - \sum_{j=1}^C y_j \log(\hat{y}_j), \quad (8)$$

$\hat{\mathbf{y}}$  and  $\mathbf{y}$  are the predicted- and target distributions, respectively, and  $C$  is the number of object classes. For Eq. 9, the parameters are defined as following:

- $z_i$ : L2-normalized feature of sample  $i$ ,  $z_i = f(x_i)/\|f(x_i)\|$
- $f(x_i)$ : Model output (pre-normalized feature vector) for input  $x_i$ .
- $y_i$ : Class label (integer) of sample  $i$ .
- $\tau$ : Temperature  $> 0$ .
- $A(i)$ : All non-self indices  $\{k \mid k \neq i\}$ ; candidates contrasted against anchor  $i$ .

- $P(i)$ : Positive indices  $\{j \in A(i) \mid y_j = y_i\}$ ; same-class samples for anchor  $i$ .
- $|P(i)|$ : Number of positives for anchor  $i$ .

#### IV. RESULTS AND PERFORMANCE COMPARISON

The evaluation of our occluded object classification models is conducted using two sub-sets of data. One subset, introduced in [15], consists of samples collected at a center frequency of 64 GHz. We extended the original dataset with an additional subset collected at a center frequency of 67 GHz. Both subsets use a 4 GHz bandwidth. This extension enables a comparative analysis of the penetration capabilities of the two frequency bands. The object collection consists of ten everyday items of similar size, which were placed individually in different orientations inside a packaging box before being scanned with the mmWave radar. The object collection contains the following items:

- Hammer
- Screwdriver
- Deodorant
- Calculator
- Water bottle
- Plastic cup
- Coiled cable
- Ball
- Mug
- Tape roll

The used objects as a collection can be seen in Fig. 6. The dataset is divided into training and test sets using the conventional 80/20 ratio. Training and testing are conducted separately with the 64 GHz and 67 GHz datasets. Our empirical evaluation identified  $\tau = 0.1$  as the best temperature value, ensuring stable training and reliable convergence. We also tested different values of  $\alpha$ , and  $\alpha = 0.4$  achieved the best overall performance across both frequencies. To demonstrate the effectiveness of our approach, we compare its overall classification accuracy with several classification models. The evaluation tables are divided into two categories. Table I presents the performance of various classification models that can directly process complex-valued radar signal input. It shows the improved classification accuracy achieved with our proposed ACCOR model. This holds for both frequency bands, with RadarCNN and SMCNet performing better on the 67 GHz data, while the Dual-stream CNN and our proposed model perform better on the 64 GHz data. Due to this inversion in performance across these models, it cannot be finally concluded that one frequency

$$\ell_\kappa = \frac{1}{|\{i : |P(i)| > 0\}|} \sum_{i: |P(i)| > 0} \left( -\frac{1}{|P(i)|} \sum_{j \in P(i)} \log \frac{\exp\left(\frac{z_i^\top z_j}{\tau}\right)}{\sum_{k \in A(i)} \exp\left(\frac{z_i^\top z_k}{\tau}\right)} \right) \quad (9)$$

with  $z_i = \frac{f(x_i)}{\|f(x_i)\|_2}$ ,  $A(i) = \{k \mid k \neq i\}$ ,  $P(i) = \{j \in A(i) \mid y_j = y_i\}$ , and temperature  $\tau > 0$ .



Fig. 6. Collection of the ten objects used in the experiments [15].

TABLE I  
OVERALL ACCURACY OF RADAR MODELS.

Model	Accuracy 64 GHz	Accuracy 67 GHz
RadarCNN [27]	90.14 %	91.80 %
SMCNet [16]	91.89 %	92.67 %
Dual-stream CNN [15]	95.15 %	92.30 %
ACCOR	<b>96.60 %</b>	<b>93.59 %</b>

band is superior in penetrating the packaging and retrieving meaningful information for all models. One possible reason is the close proximity of the two frequency bands, which differ by only 0.21 mm in wavelength (64 GHz:  $\lambda = 4.68$  mm, 67 GHz:  $\lambda = 4.47$  mm). A larger wavelength difference would likely result in a more noticeable variation in penetration capability. This is not feasible with the currently used 62–67 GHz radar sensor. However, both frequencies provide sufficient information to achieve over 90% overall classification accuracy across all models, with our approach consistently outperforming the others. Table II, however, shows the performance of image classification models, which expect RGB image input. To meet this requirement, the radar signal is split into real and imaginary parts and zero-padded for the third color channel to match the desired input dimensions. We deliberately avoided converting the data into an RGB radar map image, since this would discard phase information and reduce the representation to a real-valued image, thereby losing relevant information. We trained every model ten times with consistent seeds to ensure the statistical significance of the results. Furthermore, Table

TABLE II  
OVERALL ACCURACY OF COMMON IMAGE CLASSIFICATION MODELS.

Model	64 GHz	67 GHz
Baseline EfficientNet b0 [40]	70.83 %	55.33 %
Scaled EfficientNet b4 [40]	46.83 %	36.00 %
ResNet-18 [39]	93.36 %	89.00 %
ResNet-34 [39]	46.81 %	58.67 %
ACCOR	<b>96.60 %</b>	<b>93.59 %</b>

TABLE III  
ABLATION STUDY OF OUR PROPOSED METHOD FOR DIFFERENT VALUES OF  $\alpha$ .

ACCOR Model Setting	Accuracy 64 GHz	Accuracy 67 GHz
$\alpha = 0.6$	96.10 %	92.89 %
$\alpha = 0.5$	96.17 %	93.89 %
$\alpha = 0.4$	96.60 %	93.59 %
$\alpha = 0.3$	96.40 %	93.39 %
$\alpha = 0.2$	96.40 %	92.29 %
$\alpha = 0.1$	95.30 %	91.60 %
$\alpha = 0$ (only CE)	94.50 %	90.10 %

II shows the results of various image classification models applied to our data. ACCOR achieves higher overall accuracy compared to image classification models. ResNet-18 is the best-performing image classification model on our pseudo-image data. Generally, all image-based approaches struggle to extract the features required for reliable classification. Table III shows an ablation study of our proposed method with different weighting factors  $\alpha$ . The evaluation ranges from  $\alpha = 0.6$  to  $\alpha = 0$ , where the contrastive loss is ignored, providing an ablation to assess performance with cross-entropy loss only (0.5 is equal weighting). We observe higher accuracy overall for the 64 GHz data, suggesting that our model extracts features more effectively from this subset than from the 67 GHz data. In general, performance decreases as  $\alpha$  is reduced from 0.4 or exceeds 0.5, making these values for  $\alpha$  the ideal values for our model and highlighting the benefit of adding contrastive loss in our application. The results for  $\alpha = 0.4$  and  $\alpha = 0.5$  appear slightly contradictory. The 64 GHz band performs better with  $\alpha = 0.4$ , whereas the 67 GHz band performs better with  $\alpha = 0.5$ . These differences are, however, minor, and accuracy remains above that of SOTA models for both  $\alpha$  values. This suggests some ambiguity in the optimal  $\alpha$ , with performance peaking around these values. The best overall accuracy is achieved with  $\alpha = 0.4$ , with performance tapering off for both larger and smaller values, namely  $\alpha = 0.6$  and from  $\alpha = 0.3$ .

## V. CONCLUSION

In this work, we addressed occluded object classification for non-visual inspection in indoor settings, demonstrating that mmWave radar is a suitable sensor for this task. Our proposed ACCOR model, which integrates complex-valued CNNs, attention, and a hybrid loss, achieved state-of-the-art accuracy of 96.60% at 64 GHz and 93.59% at 67 GHz, surpassing existing radar and image-based classifiers. While the ambiguity in loss weighting highlights opportunities for further refinement, and the limited frequency range calls for broader evaluation, these results confirm the promise of complex-valued, attention-enhanced learning for mmWave

radar perception. Future work will expand to datasets with larger wavelength differences and more diverse objects, paving the way toward robust radar-based perception for industrial automation.

## REFERENCES

- [1] A. -C. Froehlich et al., "A Millimeter-Wave MIMO Radar Network for Human Activity Recognition and Fall Detection," 2024 IEEE Radar Conference (RadarConf24), Denver, CO, USA, 2024, pp. 1-5, doi: 10.1109/RadarConf2458775.2024.10548702.
- [2] P. Zhao et al., "mID: Tracking and Identifying People with Millimeter Wave Radar," 2019 15th International Conference on Distributed Computing in Sensor Systems (DCOSS), Santorini, Greece, 2019, pp. 33-40, doi: 10.1109/DCOSS.2019.00028.
- [3] Z. Pan, F. Ding, H. Zhong and C. X. Lu, "RaTrack: Moving Object Detection and Tracking with 4D Radar Point Cloud," 2024 IEEE International Conference on Robotics and Automation (ICRA), Yokohama, Japan, 2024, pp. 4480-4487, doi: 10.1109/ICRA57147.2024.10610368.
- [4] L. Senigagliesi, G. Ciattaglia, D. Disha and E. Gambi, "Classification of Human Activities based on Automotive Radar Spectral Images Using Machine Learning Techniques: A Case Study," 2022 IEEE Radar Conference (RadarConf22), New York City, NY, USA, 2022, pp. 1-6, doi: 10.1109/RadarConf2248738.2022.9764217.
- [5] J. Chen, P. Wen, G. Chen, Y. Wang, Y. Wang and J. Zheng, "Hand Gesture Recognition based on Millimeter-Wave Radar using iFormer," 2024 9th International Conference on Signal and Image Processing (ICSIP), Nanjing, China, 2024, pp. 22-26, doi: 10.1109/IC SIP61881.2024.10671474.
- [6] S. M. Kahya, M. Sami Yavuz and E. Steinbach, "HAROOD: Human Activity Classification and Out-Of-Distribution Detection with Short-Range FMCW Radar," ICASSP 2024 - 2024 IEEE International Conference on Acoustics, Speech and Signal Processing (ICASSP), Seoul, Korea, Republic of, 2024, pp. 6950-6954, doi: 10.1109/ICASSP48485.2024.10447729.
- [7] P. Wolters et al., "Unleashing HyDRA: Hybrid Fusion, Depth Consistency and Radar for Unified 3D Perception," 2025 IEEE International Conference on Robotics and Automation (ICRA), Atlanta, GA, USA, 2025, pp. 7467-7474, doi: 10.1109/ICRA55743.2025.11127412.
- [8] P. Wolters, J. Gilg, T. Teepe and G. Rigoll, "SpaRC-AD: A Baseline for Radar-Camera Fusion in End-to-End Autonomous Driving", arXiv.org, 2025.
- [9] X. Peng, M. Tang, H. Sun, L. Servadei and R. Wille, "4D mmWave Radar in Adverse Environments for Autonomous Driving: A Survey," arxiv.org, 2025.
- [10] M. Xiong, X. Xu, D. Yang and E. Steinbach, "Robust Depth Estimation in Foggy Environments Combining RGB Images and mmWave Radar," 2022 IEEE International Symposium on Multimedia (ISM), Italy, 2022, pp. 34-41, doi: 10.1109/ISM55400.2022.00011.
- [11] H. Kulhandjian, A. Davis, L. Leong, M. Bendot and M. Kulhandjian, "AI-based Human Detection and Localization in Heavy Smoke using Radar and IR Camera," 2023 IEEE Radar Conference (RadarConf23), San Antonio, TX, USA, 2023, pp. 1-6, doi: 10.1109/RadarConf2351548.2023.10149735.
- [12] X. Shuai, Y. Shen, Y. Tang, S. Shi, L. Ji and G. Xing, MilliEye: A Lightweight mmWave Radar and Camera Fusion System for Robust Object Detection. In Proceedings of the International Conference on Internet-of-Things Design and Implementation (IoTDI '21). Association for Computing Machinery, New York, NY, USA, 2021, 145–157. <https://doi.org/10.1145/3450268.3453532>.
- [13] R. Rückert, I. Ullmann, C. Herglotz, A. Kaup and M. Vossiek, "Data Compression for Close-Range Radar Imaging," in IEEE Transactions on Radar Systems, vol. 2, pp. 421-433, 2024, doi: 10.1109/TRS.2024.3387288.
- [14] S. S. Ahmed, "Microwave Imaging in Security — Two Decades of Innovation," in IEEE Journal of Microwaves, vol. 1, no. 1, pp. 191-201, Jan. 2021, doi: 10.1109/JMW.2020.3035790.
- [15] S. Hägele, F. Seguel, S. M. Kahya and E. Steinbach, "Occluded Object Classification With mmWave MIMO Radar IQ Signals Using Dual-Stream Convolutional Neural Networks," in IEEE Transactions on Radar Systems, vol. 3, pp. 789-798, 2025, doi: 10.1109/TRS.2025.3571284.
- [16] S. Hägele, F. Seguel, D. Salihu, A. Misik and E. Steinbach, "SM-CNet: Supervised Surface Material Classification Using mmWave Radar IQ Signals and Complex-valued CNNs," ICASSP 2025 - 2025 IEEE International Conference on Acoustics, Speech and Signal Processing (ICASSP), Hyderabad, India, 2025, pp. 1-5, doi: 10.1109/ICASSP49660.2025.10890769.
- [17] Y. Liu, S. Chang, Z. Wei, K. Zhang and Z. Feng, "Fusing mmWave Radar With Camera for 3-D Detection in Autonomous Driving," in IEEE Internet of Things Journal, vol. 9, no. 20, pp. 20408-20421, 15 Oct.15, 2022, doi: 10.1109/JIOT.2022.3175375.
- [18] T. Kawaguchi, K. Shinotsuka and S. Malterer, "Experimental Verification of Rainfall Impact on Sparse Array Radar," 2024 IEEE Radar Conference (RadarConf24), Denver, CO, USA, 2024, pp. 1-6, doi: 10.1109/RadarConf2458775.2024.10548312.
- [19] J. Pegoraro and M. Rossi, "Real-Time People Tracking and Identification From Sparse mm-Wave Radar Point-Clouds," in IEEE Access, vol. 9, pp. 78504-78520, 2021, doi: 10.1109/ACCESS.2021.3083980.
- [20] S. Ahmed, S. Abdullah and S. H. Cho, "Advancements in Radar Point Cloud Processing for Macro Human Movements in Healthcare and Assisted Living Domains: A Review," in IEEE Sensors Journal, vol. 24, no. 22, pp. 36287-36305, 15 Nov.15, 2024, doi: 10.1109/JSEN.2024.3452110.
- [21] G. Liao, J. Ma and F. Luo, "Human Activity Recognition by Using Enhanced Radar Point Cloud 2D Histograms and Doppler Feature Fusion," 2025 IEEE International Conference on Robotics and Automation (ICRA), Atlanta, GA, USA, 2025, pp. 11234-11241, doi: 10.1109/ICRA55743.2025.11128165.
- [22] D. Qosja, S. Wagner and D. O'Hagan, "SAR Image Synthesis with Diffusion Models," 2024 IEEE Radar Conference (RadarConf24), Denver, CO, USA, 2024, pp. 1-6, doi: 10.1109/RadarConf2458775.2024.10549257.
- [23] X. Wang, T. Ye, R. Kannan and V. Prasanna, "FACTUAL: A Novel Framework for Contrastive Learning Based Robust SAR Image Classification," 2024 IEEE Radar Conference (RadarConf24), Denver, CO, USA, 2024, pp. 1-6, doi: 10.1109/RadarConf2458775.2024.10549364.
- [24] W. Zhang, Y. Ji, W. Shao, B. Lin, C. Li and G. Fang, "A Fast 3-D Chirp Scaling Imaging Technique for Millimeter-Wave Near-Field Imaging," in IEEE Transactions on Microwave Theory and Techniques, vol. 71, no. 2, pp. 827-841, Feb. 2023, doi: 10.1109/TMTT.2022.3205926.
- [25] F. Zhang, C. Wu, B. Wang and K. J. R. Liu, "mmEye: Super-Resolution Millimeter Wave Imaging," in IEEE Internet of Things Journal, vol. 8, no. 8, pp. 6995-7008, 15 April15, 2021, doi: 10.1109/JIOT.2020.3037836.
- [26] IMAGEVK-74 4D Imaging Radar, Mini-Circuits and Vayyar, [https://www.minicircuits.com/WebStore/imagevk\\_74.html](https://www.minicircuits.com/WebStore/imagevk_74.html)
- [27] S. Hägele, F. Seguel, D. Salihu, M. Zakour and E. Steinbach, "RadarCNN: Learning-Based Indoor Object Classification from IQ Imaging Radar Data," 2024 IEEE Radar Conference (RadarConf24), Denver, CO, USA, 2024, pp. 1-6, doi: 10.1109/RadarConf2458775.2024.10548874.
- [28] Z. Huang, A. Pemasiiri, S. Denman, C. Fookes and T. Martin, "Multi-Task Learning For Radar Signal Characterisation," 2023 IEEE International Conference on Acoustics, Speech, and Signal Processing Workshops (ICASSPW), Rhodes Island, Greece, 2023, pp. 1-5, doi: 10.1109/ICASSPW59220.2023.10193318.
- [29] M. A. Maisto, M. Masoodi, R. Pierri and R. Solimene, "Sensor Arrangement in Through-the Wall Radar Imaging," in IEEE Open Journal of Antennas and Propagation, vol. 3, pp. 333-341, 2022, doi: 10.1109/OJAP.2022.3159279.
- [30] S. Huang, J. Qian, Y. Wang, X. Yang and L. Yang, "Through-the-Wall Radar Super-Resolution Imaging Based on Cascade U-Net," IGARSS 2019 - 2019 IEEE International Geoscience and Remote Sensing Symposium, Yokohama, Japan, 2019, pp. 2933-2936, doi: 10.1109/IGARSS.2019.8900569.
- [31] K. Harlow, H. Jang, T. D. Barfoot, A. Kim and C. Heckman, "A New Wave in Robotics: Survey on Recent MnWave Radar Applications in Robotics," in IEEE Transactions on Robotics, vol. 40, pp. 4544-4560, 2024, doi: 10.1109/TRO.2024.3463504.
- [32] X. Huang, N. Patel and K. P. Tsui, "Application of mmWave Radar Sensors for Autonomous Robotics Navigation," 2023 IEEE Asia-Pacific Conference on Computer Science and Data Engineering (CSDE), Nadi, Fiji, 2023, pp. 1-7, doi: 10.1109/CSDE59766.2023.10487689.
- [33] P. Meiresone, D. Van Hamme, W. Philips and T. Verbelen, "Ego-motion estimation with a lowpower millimeterwave radar on

a UAV," International Conference on Radar Systems (RADAR 2022), Hybrid Conference, Edinburgh, UK, 2022, pp. 371-376, doi: 10.1049/icp.2022.2346.

[34] Y. Li, C. Wan, X. Zhou and T. Tang, "Small-Sample SAR Target Recognition Using a Multimodal Views Contrastive Learning Method," in IEEE Geoscience and Remote Sensing Letters, vol. 22, pp. 1-5, 2025, Art no. 4007905, doi: 10.1109/LGRS.2025.3557534.

[35] C. Li, L. Du and Y. Du, "Semi-Supervised SAR ATR Based on Contrastive Learning and Complementary Label Learning," in IEEE Geoscience and Remote Sensing Letters, vol. 21, pp. 1-5, 2024, Art no. 4016405, doi: 10.1109/LGRS.2024.3458948.

[36] L. Cheng and S. Cao, "TransRAD: Retentive Vision Transformer for Enhanced Radar Object Detection," in IEEE Transactions on Radar Systems, vol. 3, pp. 303-317, 2025, doi: 10.1109/TRS.2025.3537604.

[37] A. Vaswani, N. Shazeer, N. Parmar, J. Uszkoreit, L. Jones, A. N. Gomez, Ł. Kaiser, and I. Polosukhin. Attention is all you need. In Proceedings of the 31st International Conference on Neural Information Processing Systems (NIPS'17). Curran Associates Inc., Red Hook, NY, USA, 2017.

[38] F. Seguel, D. Salihu, S. Haegele and E. Steinbach, "Complex-valued Deep Learning for WiFi-based Indoor Positioning: Method and performance," European Wireless 2024; 29th European Wireless Conference, Brno, Czech Republic, 2024, pp. 59-65.

[39] K. He, X. Zhang, S. Ren and J. Sun, "Deep Residual Learning for Image Recognition," 2016 IEEE Conference on Computer Vision and Pattern Recognition (CVPR), Las Vegas, NV, USA, 2016, pp. 770-778, doi: 10.1109/CVPR.2016.90.

[40] M. Tan and Q. V. Le, "EfficientNet: Rethinking Model Scaling for Convolutional Neural Networks," CoRR, <http://arxiv.org/abs/1905.11946>, 2019.